Available online at www.sciencedirect.com
ScienceDirect
Atmospheric Environment 42 (2008) 4185–4197
ATMOSPHERIC ENVIRONMENT
www.elsevier.com/locate/atmosenv

Sensitivity of biogenic emissions simulated by a land-surface model to land-cover representations

Lindsey E. Gulden*, Zong-Liang Yang*, Guo-Yue Niu

Department of Geological Sciences, The John A. and Katherine G. Jackson School of Geosciences, The University of Texas at Austin, 1 University Station #C1100, Austin, Texas 78712-0254, USA

Received 15 May 2007; received in revised form 11 January 2008; accepted 11 January 2008

Abstract

We evaluate the sensitivity of biogenic emissions simulated by a land-surface model (LSM) to different representations of land-cover vegetation. We drive the community land model on a 0.1° grid over Texas, USA, from 1993 to 1998 using bilinearly interpolated North American Regional Reanalysis data. Two land-cover datasets provide the starting point for analysis: (1) a satellite-derived vegetation and soil-color database and (2) a vegetation-distribution dataset derived from ground surveys. These datasets help us to qualitatively characterize the uncertainty in land-cover representations. We systematically vary the datasets to examine the sensitivity of modeled emissions to variation in representation of bare-soil fraction, vegetation-type distribution, and phenology.

Different datasets' representation of vegetation-type distribution leads to simulated mean statewide total biogenic emissions that vary by a factor of 3. Variation in specified bare-soil fraction causes simulated statewide average emissions that vary by a factor of 1.7. Scaling leaf area index values within reasonable bounds causes a near-linear change in simulated emissions. Differences in simulated values are the largest for major metropolitan regions and for eastern and central Texas, where biogenic emissions are the highest and where tropospheric ozone pollution is a significant concern. Changing bare-soil fraction alters simulated vegetation temperature and consequently indirectly affects modeled emissions ($\leqslant$16% of inherent emissions capacity). Our estimates of the model sensitivity to land-cover representation are consistent with those for other regions.

Keywords: Biogenic emissions; Sensitivity analysis; Land-surface model; Air quality; Land-cover dataset; Vegetation; BVOCs; Isoprene; Monoterpene

1. Introduction

Realistic simulation of biogenic emissions is a shared goal of climate scientists, the environmental engineering community, and air-quality policy-makers. Biogenic volatile organic compounds (BVOCs) were first recognized as a key contributor to the formation of photochemical smog and were subsequently identified as actors in diverse climatic processes. In addition to their role in the production of tropospheric ozone, BVOCs condense to form secondary organic aerosols, which alter Earth's radiative balance (Kavouras et al., 1998; Claeys et al., 2004, Kroll et al., 2006) and serve as cloud

*Corresponding authors. Tel.: +1 512 471 3824.
E-mail addresses: gulden@mail.utexas.edu (L.E. Gulden), liang@mail.utexas.edu (Z.-L. Yang).

1352-2310/$ - see front matter © 2008 Elsevier Ltd. All rights reserved.
doi:10.1016/j.atmosenv.2008.01.045

condensation nuclei (Andreae and Crutzen, 1997). BVOCs are a non-negligible component of the global carbon cycle (e.g., Altshuller, 1991; Guenther, 2002).

Realistic representation of biogenic emissions within land-surface models (LSMs) is important for numerical weather forecasts, climate simulations, and the generation of accurate air-quality forecasts. Because BVOCs transmit information about surface conditions between the land surface and the atmosphere, realistic simulation of the spatial distribution and magnitude of BVOC fluxes to the atmosphere likely improves the quality of simulated atmospheric conditions. Most research addressing how environmental change alters biogenic emissions and air quality has used meteorological model output to drive free-standing, task-specific biogenic emissions models and air-quality models (e.g., Tao et al., 2003). Synchronous coupling of consistent meteorological models, atmospheric-chemistry models, and LSMs (e.g., Grell et al., 2005) has recently provided geoscientists with an improved capacity to simulate feedbacks between BVOC fluxes and other environmental components (Levis et al., 2003). LSM-simulated biogenic emissions such as those used within synchronously coupled systems inherit all sources of uncertainty associated with traditional biogenic emissions models (e.g., GloBEIS [Yarwood et al., 1999]) as well as additional sources of uncertainty unique to LSMs (e.g., coarse horizontal grid resolution and simplistic representation of vegetation [Gulden and Yang, 2006; Gulden et al., 2007]).

Regardless of the type of model used, simulated BVOC flux estimates are notoriously uncertain. Guenther (1997) used six land-cover datasets to estimate the emission potential (units: $\mu g\,C\,m^{-2}\,h^{-1}$ at 30 °C and 1000 $\mu mol\,photons\,m^{-2}\,h^{-1}$) of the contiguous United States and found a 3–5-fold difference in estimated inherent emission capacity. Other researchers, looking at sources of uncertainty ranging from meteorological inputs to vegetation-species distribution, have asserted that uncertainty in BVOC flux estimates ranges from a factor of 1.5 to more than 10, depending on the species of BVOC (e.g., Simpson et al., 1999; Smiatek and Bogacki, 2005). Such uncertainty compromises air-quality simulations that depend on biogenic emissions estimates. Byun et al. (2005) used a satellite-derived dataset and the parent dataset of the ground-survey-derived dataset used here (Wiedinmyer et al., 2001) to show that selection of land-cover dataset can lead to a 10 ppb difference in simulated ozone concentrations for the metropolitan area surrounding Houston and Galveston, Texas, USA.

Although the true level of uncertainty in LSM land-cover datasets is difficult to quantify because of a dearth of observations (e.g., Simpson et al., 1999; Wiedinmyer et al., 2001), cursory examination of peer-reviewed literature introducing LSM-formatted land-cover datasets highlights the range of representations that have been deemed reasonable by the community (e.g., Bonan et al., 2002a; Wiedinmyer et al., 2001; Lawrence and Chase, 2007).

In models that employ the Guenther et al., 1995 biogenic emissions algorithm or a close derivative (e.g., Levis et al., 2003), BVOC flux is a function of biomass, vegetation type, and environmental variation. A land-cover dataset's specified percentage of bare soil and the prescribed phenological variation determine the quantity of biomass on the modeled land surface. The land-cover dataset also determines both the types and percent composition of vegetation in a grid cell.

From all potential sources of uncertainty (Beck, 1987; Wagener and Gupta, 2005) in LSM-simulated biogenic emissions (e.g., lack of process understanding, oversimplification of physical processes, representation of heterogeneous vegetation with a limited number of plant functional types, model parameter uncertainty, uncertainty in meteorological forcing data, etc.), we focus here only on uncertainty that results from variation between datasets that specify land-cover characteristics. We perform a simple sensitivity analysis (Saltelli et al., 2000) to quantitatively and qualitatively attribute variation in LSM-simulated BVOC flux to different land-cover datasets.

We created several "cross-pollinated" land-cover datasets for the state of Texas, USA. Starting with a satellite-derived land-cover dataset (Lawrence and Chase, 2007) and a ground-survey-derived land-cover dataset (Wiedinmyer et al., 2001; Gulden and Yang, 2006), we systematically varied, at each grid point in our model domain, the percent vegetated area, the vegetation distribution, and the magnitude of the specified phenology. To assess the sensitivity of LSM-simulated biogenic emissions to the representation of surface vegetation, we used the hybrid datasets to initialize offline LSM runs. We examined the relative importance of the direct and indirect means by which divergent land-cover representations change simulated BVOCs.

We employ the National Center for Atmospheric Research's community land model version 3 (CLM) (Oleson et al., 2004; Bonan et al., 2002b). CLM is a land-surface model (LSM) that incorporates a BVOC-flux module (Levis et al., 2003) founded on the work of Guenther et al. (1995). CLM is representative of LSMs commonly used in climate modeling. This research contributes to efforts to quantify the uncertainty associated with LSM-simulated biogenic emissions that is directly attributable to land-cover dataset (e.g., Guenther et al., 2006).

2. Model, datasets, and methods

2.1. Representation of vegetation and biogenic emissions in CLM

CLM represents land cover as a mosaic of plant functional types (PFTs) (Bonan et al., 2002a). Each grid cell in the model domain is assigned a percentage of vegetated area; the vegetated area is further subdivided into four or fewer PFTs. The standard CLM, which uses static ecosystem dynamics, calculates daily variation in leaf area index (LAI) by linearly interpolating between prescribed monthly LAI values. Each PFT within model grid cell is assigned a unique LAI value for each month. Foliar density (the weight of dry leaf matter per unit area of ground covered by the PFT) is the product of LAI and specific leaf area (m^2 leaf g^{-1} dry leaf matter). Although the static ecosystem dynamics of CLM allow LAI and stem area index (SAI) to vary seasonally, their seasonal cycle remains constant year to year.

CLM represents emission of isoprene, monoterpene, other volatile organic compounds, other reactive volatile organic compounds, and biogenic carbon monoxide (Levis et al., 2003; Guenther et al., 1995). For a given PFT, CLM simulates the flux of BVOC type i as

$$F_i = \varepsilon_i D \gamma_{\mathrm{PAR}} \gamma_T \quad (1)$$

where F_i is the flux to the atmosphere of BVOC type i (units: $\mu g\,C\,m^{-2}\,h^{-1}$); D is the foliar density (units: g dry leaf matter (gdlm) m^{-2} of ground covered by the PFT), which is a scalar function of LAI; ε_i is a PFT-specific emission capacity for BVOC type i (units: $\mu g\,C\,gdlm^{-1}\,h^{-1}$); γ_T is a dimensionless, nonlinear function of canopy temperature that modulates BVOC emissions; and γ_{PAR} is a dimensionless, nonlinear function of photosynthetically active radiation reaching the leaf surface that modulates isoprene emissions (for non-isoprene BVOCs, we assume $\gamma_{\mathrm{PAR}} = 1$).

2.2. Baseline land-cover datasets

Two source datasets provided the starting point for our analysis. The first is a 1-km PFT-distribution dataset developed from a ground-referenced, species-based dataset in which each grid cell contained between 1 and 115 of approximately 300 possible vegetation species (henceforth the "survey-derived dataset"). Wiedinmyer et al. (2001) describe the original species-based dataset; Gulden and Yang (2006) describe the conversion of the dataset to CLM format. The second raw dataset was derived from moderate resolution imaging spectroradiometer (MODIS) and advanced very high resolution radiometer (AVHRR) satellite images (Lawrence and Chase, 2007) and contains 5-km resolution PFT distribution, plant phenological and structural parameters (LAI, SAI, height of canopy top and bottom), and soil-color information (henceforth the "satellite-derived dataset"). We interpolated both datasets to a uniform 0.1° grid. We used the two original datasets as parents from which we derived five unique, hybridized land-cover datasets. We used the hybridized datasets in lieu of the two originals such that we could more rigorously examine the sensitivity of the model to specific aspects of land-cover representation (i.e., PFT distribution, bare-soil fraction, magnitude of specified phenology).

Fig. 1 shows that the survey-derived dataset identifies 44.5% of the area of Texas as bare soil; the satellite-derived dataset labels 20.0% of Texas as bare soil. The difference in bare-soil fraction is especially pronounced in central and eastern Texas. Trees cover 20.3% of Texas in the survey-derived dataset; in the satellite-derived dataset trees cover 10.7%. Introduced in the peer-reviewed literature, both datasets have been deemed reasonable representations of reality by the scientific community and are used for both scientific and engineering purposes (P. Lawrence, personal communication; e.g., Junquera et al., 2005). Variations in simulated biogenic emissions that result from the use of these two datasets help us to qualitatively characterize the uncertainty in LSM-simulated emissions that stem from uncertain land-cover representations.

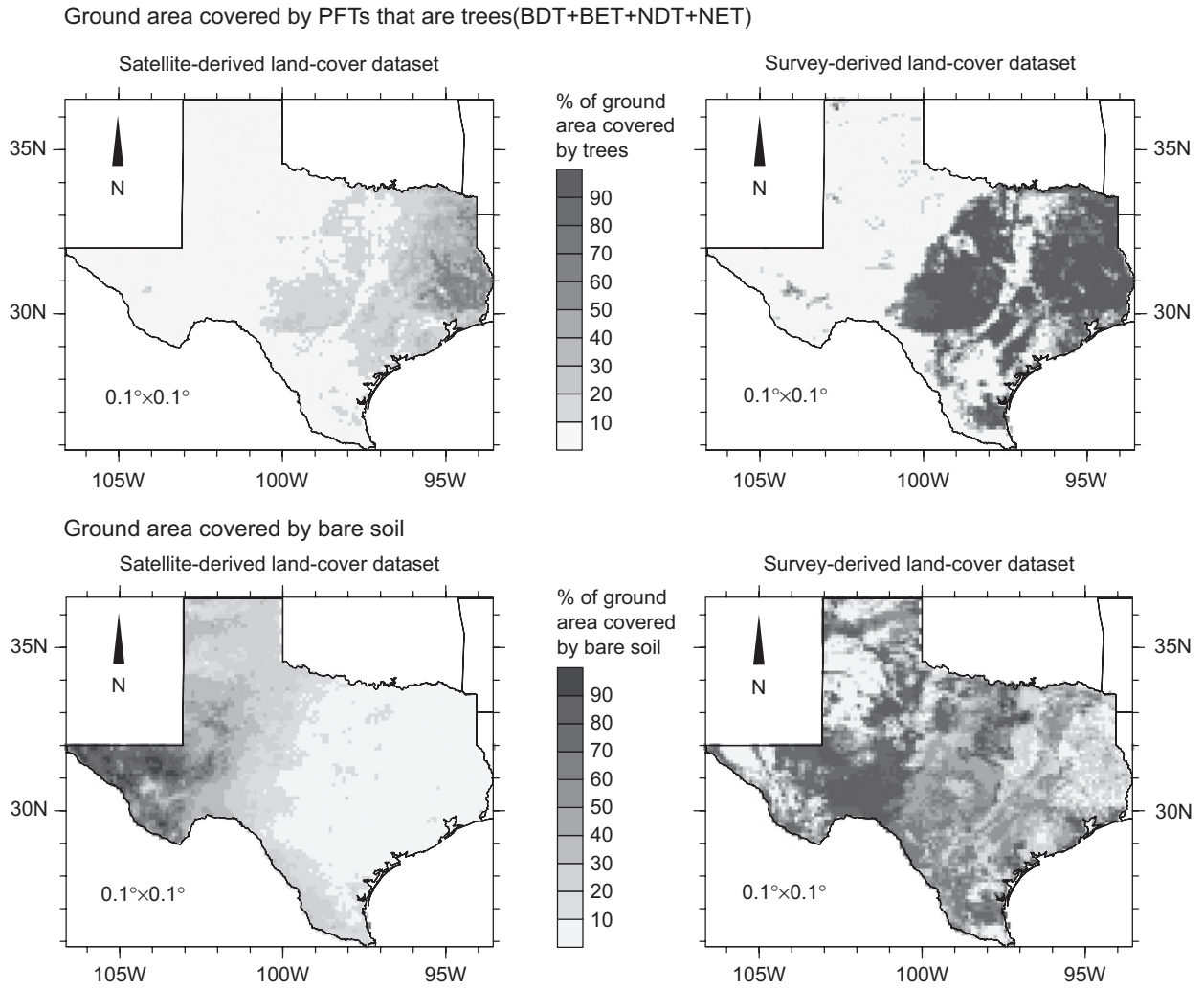

Fig. 1. Summary of the biogenic emissions—relevant differences between the satellite-derived land-cover dataset and the survey-derived land-cover dataset.

2.3. Modified datasets

The original survey-derived dataset specifies only PFT fraction; it contains no phenological information. Before creating the hybrid datasets, we transformed the satellite-derived phenological parameters for use with the survey-derived PFT fractions. For a given grid cell, the satellite-derived dataset contains LAI and stem area index (SAI) information only for the PFTs identified as being present in that location. Because the specified vegetation distributions differ between the satellite- and survey-derived datasets, we could not directly combine the satellite-derived LAI and SAI with the survey-derived PFT distribution data. To ensure that LAI and SAI were defined at all model grid points for all PFTs (as required by CLM), we used the area-weighted, longitudinal average of the satellite-derived PFT parameters. Vegetation biomass in the state of Texas exhibits a very strong west–east gradient: an area-weighted average along lines of longitude was deemed more appropriate than a statewide average, a latitudinal average, or another averaging method.

The satellite-derived dataset does not identify broadleaf evergreen trees (BETs) or broadleaf evergreen shrubs (BESs) in Texas; it contains neither LAI nor SAI information for BET and BES. We defined the LAI and SAI of BET for all months as the June–July–August (JJA) average of

the longitudinally averaged LAI and SAI for broadleaf deciduous trees. We defined LAI and SAI for BES for all months as the JJA average of broadleaf deciduous shrubs. Needleleaf evergreen shrubs (NESs) and temperate needleleaf deciduous trees (NDTs) do not exist in the standard CLM, but they do exist in the survey-derived dataset (Gulden and Yang, 2006). We defined the LAI and SAI of NES as identical to those of BES. LAI and SAI for NDT were defined using the LAI and SAI of needleleaf evergreen tree. Because there are so few NDTs in Texas, we neglected any error caused by spuriously high NDT biomass in wintertime. Our method for defining LAI and SAI for each PFT, for each site, and for each month for the survey-based dataset did not introduce significant error: statewide BVOC flux estimates derived using the dataset with the satellite-derived PFTs, satellite-derived bare soil, and the longitudinally averaged, satellite-derived phenological parameters were consistently within 1% of estimates derived using the original satellite-derived dataset (results not shown).

We created three pairs of hybrid datasets, designing them to facilitate a clean comparison of the effect on biogenic emissions of two different realizations of a single descriptor of land-surface vegetation.

2.3.1. Dataset pair 1: PFT-SURVEY and PFT-SATELLITE

The fraction of the vegetated area covered by each PFT controls the spatial distribution and magnitude of a dataset's inherent BVOC flux: trees emit BVOCs at a rate often an order of magnitude greater than the emission rate of grasses and crops. The first pair of hybrid datasets isolated the effect of uncertainty in PFT distribution on simulated BVOC flux. The pair differed only in its PFT distribution. Derivative dataset PFT-SURVEY represents vegetation composition with the survey-derived PFT distribution. PFT-SATELLITE uses the satellite-derived PFT distribution. Both use the satellite-derived, longitudinally averaged phenological parameters and the percent bare soil specified in the satellite-derived dataset.

2.3.2. Dataset pair 2: BARE-SURVEY and BARE-SATELLITE

The partitioning of a grid cell between vegetated area and bare soil helps determine a grid cell's biomass density and affects the modeled energy and water balances. When all else is equal, a greater amount of biomass increases BVOC flux. The second set of derivative datasets allowed us to examine the sensitivity of modeled biogenic emissions to the range of realistic assessments of bare-soil fraction. The pair differed only in its bare-soil fraction. Dataset BARE-SURVEY uses the percent bare-soil specified in the survey-derived dataset; BARE-SATELLITE uses the percent bare-soil specified by the satellite-derived dataset. Both use the satellite-derived, longitudinally averaged phenological parameters; both use the survey-derived PFT distribution. (It is important to note that, although their bare-soil fraction differs, the percent of the vegetated area covered by a given PFT remains constant between the two datasets.) BARE-SATELLITE is more densely vegetated than BARE-SURVEY, especially in central and eastern Texas. Note that BARE-SATELLITE and PFT-SURVEY are identical.

2.3.3. Dataset pair 3: LAI × 0.5 and LAI × 1.5

CLM calculates BVOC flux as a linear function of biomass density, which is a scalar multiple of the PFT's LAI. To simulate uncertainty in the magnitude of phenological parameters, we modified the LAI and SAI values in the original satellite-derived dataset to create artificial datasets with underestimated and overestimated LAI and SAI values. We uniformly scaled the satellite-derived LAI and SAI values by 0.5 to create the derived dataset LAI × 0.5 and multiplied the satellite-derived LAI and SAI values by 1.5 to create LAI × 1.5. Both datasets used the satellite-derived PFT distribution and the satellite-derived vegetation fraction information. LAI × 0.5 approximates the lower bound of realistic LAI values, and LAI × 1.5 is an estimate of a reasonable upper bound for realistic LAI values. These bounds are consistent with the range of LAI values presented in the literature (e.g., Tian et al., 2004). Because the satellite-derived PFT distribution was used for all three datasets, the phenological parameters in both LAI × 0.5 and LAI × 1.5 were taken directly from the original satellite-derived phenological data (i.e., they were not longitudinally averaged).

Table 1 summarizes the characteristics of the three pairs of datasets. Hereafter, model runs will be referred according to their land-surface dataset name (e.g., "PFT-SATELLITE" will be used to mean "the model run that employed PFT-SATELLITE as its input land-cover dataset").

Table 1
Summary of source data used to create derivative dataset pairs

	Pair 1		Pair 2		Pair 3	
	PFT-SURVEY	PFT-SATELLITE	BARE-SURVEY	BARE-SATELLITE	LAI × 1.5	LAI × 0.5
PFT distribution	Survey-derived	Satellite-derived	Survey-derived	Survey-derived	Satellite-derived	Satellite-derived
Bare soil fraction	Satellite-derived	Satellite-derived	Survey-derived	Satellite-derived	Satellite-derived	Satellite-derived
Phenology	Satellite-derived; longitudinally averaged	Satellite-derived; longitudinally averaged	Satellite-derived; longitudinally averaged	Satellite-derived; longitudinally averaged	Original satellite-derived, uniformly scaled by 1.5	Original satellite-derived, uniformly scaled by 0.5

2.4. Model run parameters

North American Regional Reanalysis (NARR) data (Mesinger et al., 2006) provided meteorological input forcing. We used bilinear interpolation to convert the NARR data from their original 32 km grid to a 0.1° grid coincident with the land-surface datasets. All runs represented the period from 1 January 1993, to 1 January 1999. We analyzed model output from 1 January 1995 to 1 January 1999, a period spanning both a weak La Niña event and a strong El Niño event.

For all experiments, we used region-specific, PFT-specific emissions capacities. The emissions capacities were developed using a ground-referenced, species-based dataset (Wiedinmyer et al., 2001) and its CLM-compatible counterpart (Gulden and Yang, 2006). The CLM-compatible dataset is the survey-based dataset used as one of the two "raw" datasets.

All runs employed static ecosystem dynamics and used CLM-standard values for top and bottom heights of the canopy, both of which are spatially and temporally constant and vary only between PFTs. The satellite-derived dataset provided soil color for all simulations; soil texture was defined using the 5-min CLM-standard soil texture data.

3. Results

As expected, LSM-simulated biogenic emissions are sensitive to land cover: significant variation in model output can be directly attributed to uncertainty in land-cover dataset. We use the mean scale factor to measure change in model response that is directly attributable to a change in a specific vegetation parameter (e.g., PFT distribution). The scale factor for a given grid cell is time average ratio of BVOC flux estimates for a pair of runs. The mean scale factor is the domain average scale factor. Table 2 summarizes the results described in the following Sections 3.1–3.3 and provides additional information regarding regional differences in scale factors.

3.1. Sensitivity to representation of PFT distribution

Estimates of the statewide mean monthly BVOC flux derived from PFT-SURVEY were on average 3 times as great as those derived by PFT-SATELLITE (Fig. 2) (i.e., the mean scale factor is 3.0). This difference is the greatest during summer, when the difference between tree biomass and herbaceous biomass is the greatest.

Fig. 3 shows the spatial distribution of the differences in monthly mean JJA BVOC emissions, averaged over the period of analysis. The mean scale factor varies considerably between regions: in west Texas, where biogenic emissions are relatively low, the mean scale factor is 2; in central Texas (including San Antonio and Austin) it is ~6.

Because the survey-derived dataset was created using a suite of smaller, ground-referenced datasets, the survey-derived PFT distribution (used in PFT-SURVEY) may better represent reality than does the PFT distribution used in PFT-SATELLITE. However, the survey-derived dataset likely overestimates the percentage of trees in central Texas (Gulden and Yang, 2006). "Reality" probably lies somewhere between the two representations.

Table 2
Regional variation in the mean emission scale factor[a]

	Pairs of land-cover datasets[b]			
	PFT-SURVEY/ PFT-SATELLITE	BARE-SATELLITE/ BARE-SURVEY	LAI × 1.5/Baseline satellite-derived	Baseline satellite-derived/LAI × 0.5
Entire state of Texas				
Mean	3.0	1.7	1.5	2.0
Range	2.6–3.2	1.6–1.7	1.5–1.5	1.9–2.0
East Texas (east of −99.5°E)				
Mean	3.2	1.7	1.5	2.0
Range	2.7–3.5	1.6–1.7	1.5	1.9–2.0
West Texas (west of −99.5°E)				
Mean	2.0	1.7	1.5	2.0
Range	1.7–2.3	1.6–1.7	1.4–1.5	1.9–2.1
Houston[c]				
Mean	3.3	1.9	1.4	2.0
Range	2.4–3.8	1.8–1.9	1.4–1.5	1.9–2.0
Dallas/Fort Worth[d]				
Mean	4.6	3.3	1.5	2.0
Range	3.5–5.3	3.1–3.5	1.4–1.5	1.9–2.0
Central Texas (San Antonio, Austin)[e]				
Mean	5.9	1.9	1.5	2.0
Range	5.1–6.3	1.8–1.9	1.5	1.9–2.0

[a]The "scale factor" is the regional average ratio of BVOC flux estimates for a pair of runs. Monthly mean total BVOC flux estimates were calculated for each 0.1° × 0.1° model grid cell for each month of the simulation period (1995–1998). For instance, in the PFT-SURVEY/PFT-SATELLITE column, the model run that used the PFT-SURVEY dataset produced monthly mean flux estimates that were on average 3.0 times as great as those produced by the run using the PFT-SATELLITE data.

[b]Column headings are the land-cover datasets used in each of the two paired runs.

[c]Houston metropolitan area defined as −94.6°E to −96.0°E and 29.15°N to 30.35°N.

[d]Dallas/Fort Worth metropolitan area defined 32.40°N to 33.40°N and −96.35°E to −97.7°E.

[e]"Central Texas" (spanning both the approximate Austin and San Antonio metropolitan areas) defined as the land between −97.45°E to −99.0°E and 29.15°N to 30.75°N.

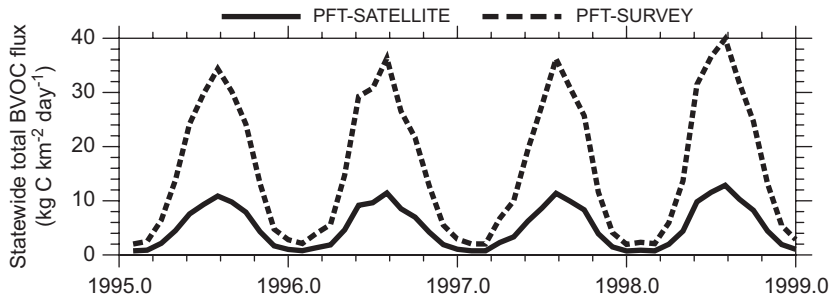

Fig. 2. Time series of BVOC flux generated by the run using PFT-SATELLITE and the run using PFT-SURVEY (flux is the monthly average, statewide total flux).

3.2. Sensitivity to representation of bare-soil fraction

The statewide total BVOC flux simulated by BARE-SATELLITE is on average 1.7 times as large as that simulated by BARE-SURVEY. Fig. 4 provides the time series of the monthly statewide total BVOC flux over the period of analysis.

Fig. 5 shows the differences in the spatial distribution of the mean JJA BVOC flux over the study period. The mean scale factor associated with bare-soil fraction does not vary by region as much as does the mean scale factor associated with PFT distribution; however, the Dallas–Fort Worth metropolitan area has a considerably higher

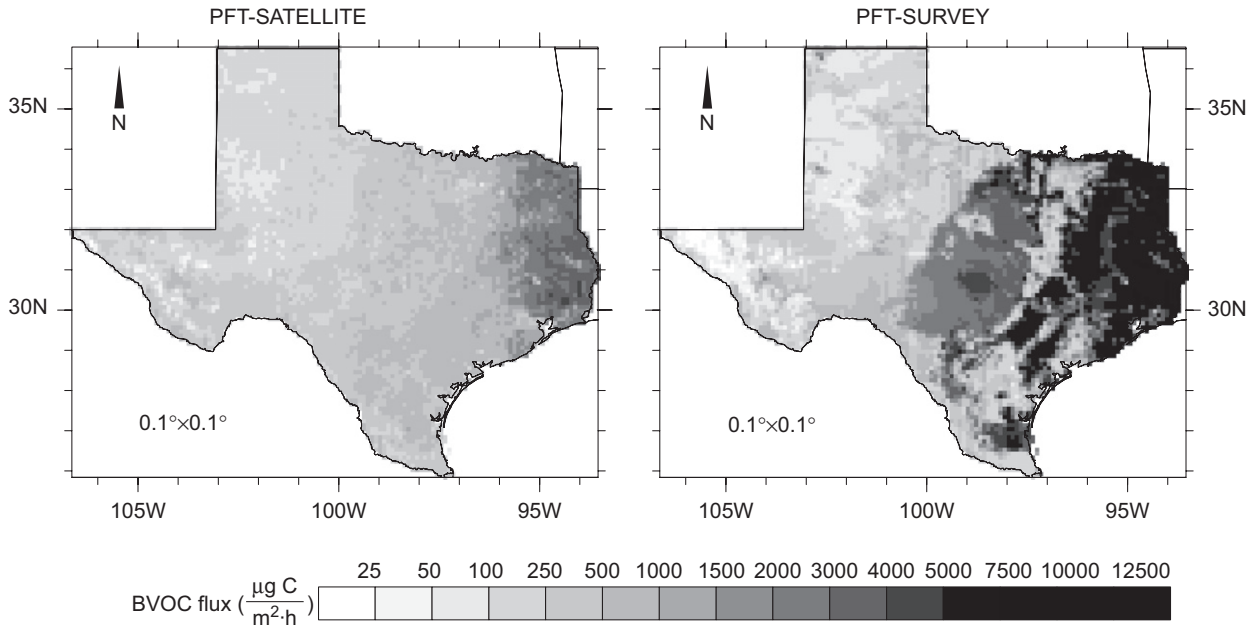

Fig. 3. Comparison of flux estimates from PFT-SATELLITE and PFT-SURVEY: June–July–August mean BVOC flux, averaged over the analysis period (1995–1998).

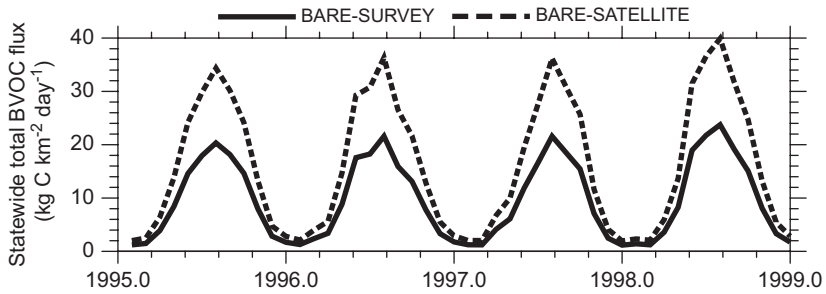

Fig. 4. Time series of BVOC flux generated by the run using BARE-SATELLITE and the run using BARE-SURVEY (Flux is the monthly average, statewide total flux).

uncertainty associated with bare-soil fraction than do other regions (mean scale factor = 3.3).

The satellite data gathers bare-soil fraction from a near-nadir perspective and is therefore arguably more in agreement with the "viewpoint" of the LSM. It is reasonable to assume that the bare-soil fraction derived from the satellite images is closer to reality, but this assertion is difficult to validate.

3.3. Sensitivity to magnitude of specified phenology

We expect that, as biomass increases, light-activated biogenic emissions decrease in increasingly shaded regions of the canopy. However, when LAI increases, a larger area of leaves receives solar radiation. When shading effects are combined with nonlinear canopy-temperature controls on emissions, it is not clear whether increasing biomass causes a corresponding linear increase in biogenic emissions.

CLM represents canopy temperature (as functions of sensible and latent heating and cooling processes) and canopy shading processes (as a function of LAI and SAI), both of which may vary nonlinearly as LAI increases. Biogenic emissions in CLM depend on environmental modulation factors γ_{PAR} and γ_T, which are nonlinear functions of radiation reaching the canopy and canopy temperature (Fig. 6). Because of these process representations, CLM has the potential to help us identify

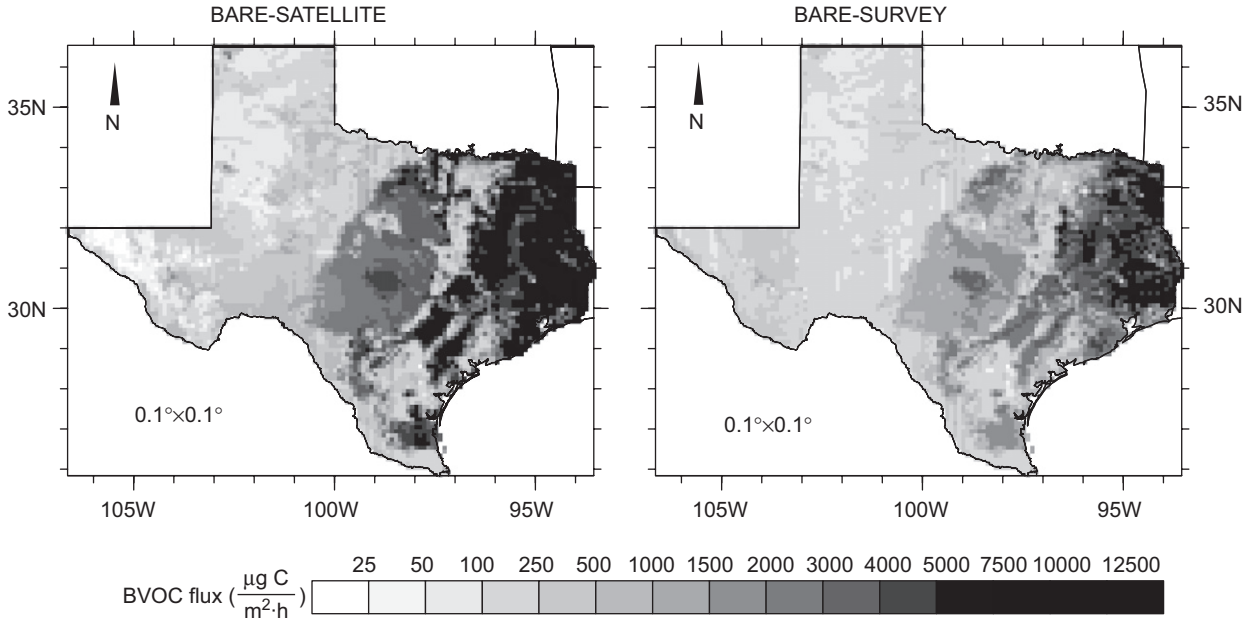

Fig. 5. Comparison of flux estimates from BARE-SATELLITE and BARE-SURVEY: June–July–August mean BVOC flux, averaged over the analysis period (1995–1998).

whether changing canopy shading and changing canopy temperature are significant controls on biogenic emissions as LAI varies.

The mean scale factor for the dataset pair made up of the LAI × 1.5 and the "raw" original satellite-derived dataset is ~1.5. The baseline dataset produces an estimate that is on average 2 times that of LAI × 0.5. Fig. 7 compares estimates obtained from LAI × 0.5 and LAI × 1.5 to the baseline run. Regional differences in mean scale factor are negligible (Table 2). The linear functional relationship between model biomass and modeled BVOC flux (Eq. (1)) causes a coincident, nearly linear scaling of the model-simulated BVOC flux when LAI and SAI are scaled. In the model (although perhaps not in nature), biogenic emissions are more sensitive to changes in biomass than to consequent changes in canopy-shaded fraction or canopy temperature.

In the case of LAI indirect effects on biogenic emissions modulated by the environmental modulation factors γ_T and γ_{PAR} are relatively insignificant. Monthly average values of γ_T remained stable; γ_{PAR} did change slightly between LAI runs, but that change was not significant (results not shown). Whether CLM adequately represents canopy temperature and canopy shading processes as functions of changing LAI remains an open research question:

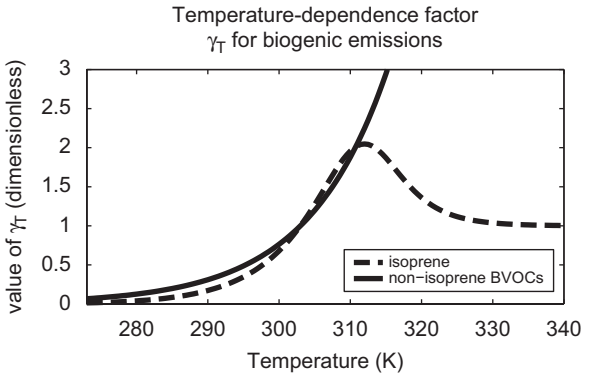

Fig. 6. Functions governing the environmental modulation factor γ_T for isoprene and non-isoprene BVOCs. γ_T allows CLM-simulated biogenic emissions to respond to variations in leaf temperature (Eq. (1)).

to our knowledge, relatively little evaluation of these parameterizations has been done.

3.4. Indirect effect of land-cover representation on biogenic emissions

PFT distribution, bare-soil fraction, and magnitude of phenological parameters all exert indirect control on the actual CLM3-simulated BVOC flux; however, the magnitude of each effect varies. Fig. 8a shows the time series of γ_T for isoprene for

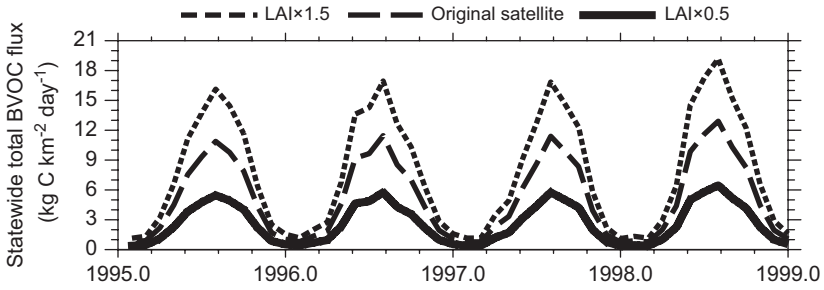

Fig. 7. Time series of BVOC flux generated by the run using LAI × 0.5, the original satellite-derived land-cover dataset, and LAI × 1.5. (Flux is the monthly average, statewide total flux.)

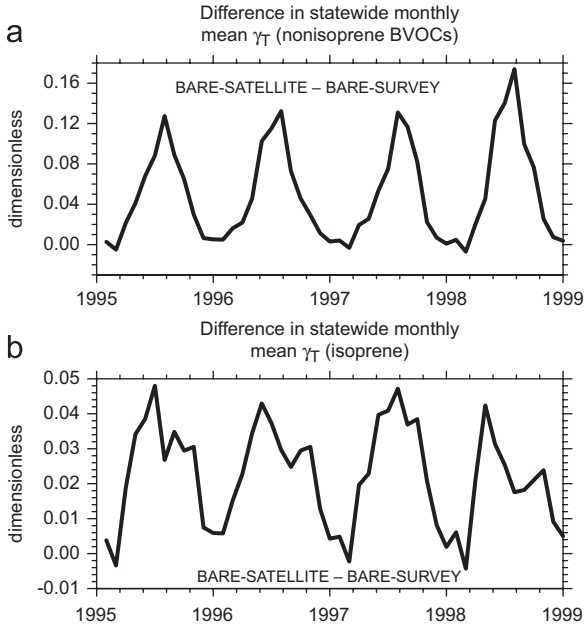

Fig. 8. Comparison of the leaf-temperature emission-modulation factors calculated by BARE-SURVEY and BARE-SATELLITE for both isoprene and non-isoprene BVOCs. Both panels show BARE-SATELLITE less BARE-SURVEY. On average, leaf temperature simulated by BARE-SATELLITE was higher than that simulated by BARE-SURVEY.

BARE-SURVEY and BARE-SATELLITE; Fig. 8b shows the corresponding time series for γ_T for non-isoprene BVOCs. Bare-soil fraction has the greatest impact on modeled leaf-surface temperature (and hence on γ_T). The higher mean leaf-surface temperature simulated by BARE-SATELLITE caused an increase in total modeled isoprene flux of up to 5% of inherent BVOC flux when compared to BARE-SURVEY. The difference in simulated vegetation temperature was responsible for an increase in total non-isoprene flux of up to 16% of the inherent BVOC flux. This is particularly important in the needleleaf evergreen forests of eastern Texas, where nonmethane biogenic hydrocarbon emissions are, at least in the model, dominated by non-isoprene BVOCs. Whether such indirect variation is representative of natural processes remains an open question.

The difference between the γ_T modulation factors for both isoprene and non-isoprene BVOCs that were calculated by LAI × 0.5 and LAI × 1.5 was in all cases $<1\%$ (results not shown). PFT-SURVEY tended to simulate slightly higher vegetation temperatures that PFT-SATELLITE. Model γ_T values were correspondingly higher: PFT-SATELLITE γ_T for non-isoprene BVOCs ranged from 1% greater to 4% less than the corresponding γ_T calculated by PFT-SURVEY. Differences between γ_T for isoprene between PFT-SATELLITE and PFT-SURVEY were between 1% and 2%.

4. Discussion

The representation of vegetation characteristics is by no means the only source of uncertainty in LSM-simulated biogenic emissions. Even if a land-cover dataset perfectly describes the "true" land-cover distribution and biomass density of a landscape, in nature, spatial variation of the species composition of can vastly alter the landscape's inherent biogenic emission flux (e.g., Guenther et al., 1994; Guenther, 1997). LSMs, including CLM, may fail to accurately simulate canopy temperature or the PAR reaching the leaf surface. Even if LSMs were to represent the "true" grid-cell average state variables, the nonlinearity of the response of BVOCs to environmental variation makes model error sensitive to subgrid-scale variation. Error in leaf-level species-based emission capacity measurements, interspecies and intraspecies variation (e.g., Funk et al., 2005) in biogenic emissions, the unproven

universal applicability of the Guenther et al. (1995) algorithm (e.g., Schuh et al., 1997), and the omission from the CLM version of the emission algorithm of factors important to emissions (such as leaf age [e.g., Zhang et al., 2000; Guenther et al., 2006]) all contribute additional uncertainty to LSM-generated BVOC fluxes. Consequently, any projection of future biogenic emissions derived from LSMs, either offline or coupled to climate models, should be viewed only as a very rough estimate.

The statewide total BVOC flux estimates that results from variation in the three vegetation descriptors examined varies by up to a factor of 3; however, the range of estimates varies significantly by region. Sensitivity of simulated emissions to the use of different land-cover datasets is the highest in regions where BVOC emissions are of the greatest concern: mean scale factors are the largest in central and eastern Texas (east of −99.5°E), where wooded and forested landscapes ensure that BVOC flux is relatively high and where tropospheric ozone pollution is a primary concern for air-quality managers. It is also worth noting that a mean scale factor of 3.2 in eastern Texas corresponds to a much larger actual difference in the mass of BVOCs emitted than would a mean scale factor of 3.2 in western Texas, where biomass density is low and tree cover is sparse. On first-order examination, range of simulated emissions values is particularly large in the major metropolitan regions of the state (see Table 2).

Uncertainty in PFT distribution is the largest source of land-cover-related variation in LSM-simulated biogenic emissions. BVOC emissions estimates within LSMs and their coupled models of the atmosphere will benefit if future land-cover data acquisition projects focus their efforts on precisely quantifying the bare-soil fraction and on the partitioning of the vegetated area between trees and grass. Of secondary—but certainly non-negligible—importance is to improve our confidence in observed estimates of the quantity of biomass present on the ground, which is determined by the percent vegetated area and by the magnitude and seasonality of leaf phenology, the latter of which we did not examine here (see Gulden et al., 2007).

This study examines only the monthly mean variation in BVOC flux, emission modulation factors, and model state variables. Divergent representations of the land surface may significantly alter estimates of the diurnal cycles of emission modulation factors, canopy state variables, and, consequently, BVOC emissions. Examination of uncertainty at a finer temporal resolution is warranted.

Use of static ecosystem dynamics, as is done in this study, considerably underestimates the true variation in biogenic emissions (Gulden et al., 2007). When employing a dynamic vegetation module that updates changes in maximum LAI once a year and allows daily variation in the fraction of the maximum LAI in response to environmental conditions, Levis et al. (2003) found that interannual variation in the total BVOC flux exceeded 29% during a 10 yr fully coupled climate simulation. Gulden et al. (2007) showed that, the absolute average departure from the monthly mean (max) BVOC flux was 22.4% (137%) when phenology was allowed to respond to the short-term environmental variation.

Our estimates of the sensitivity of simulated biogenic emissions, which focus on only one source of potential error in LSM-simulated BVOC flux and which we derived from observations-based land-cover datasets, are of the same order of magnitude as previous estimates (e.g., Simpson et al., 1999; Hanna et al., 2005).

5. Summary and conclusions

We conclude the following: (1) Differences in the representation of land-surface vegetation in the state of Texas, USA, can result in estimated monthly mean total biogenic emissions that differ by up to a factor of 3. (2) Distribution of PFTs contributes most to this variation. The ground-survey-derived PFT distribution resulted in statewide monthly mean BVOC fluxes that were an average of 3 times as large as the estimates produced by a run using a satellite-derived PFT distribution. (3) Divergent representations of bare-soil fraction significantly contribute to variation in simulated BVOC flux: a run using satellite-derived bare-soil fraction produced BVOC estimates 1.7 times as great as a run using the bare-soil fraction from the less-densely vegetated ground-survey-derived dataset. (4) Scaling LAI within reasonable bounds (50–150% of the satellite-derived estimates) caused a nearly linear decrease and increase, respectively, of simulated biogenic emissions. (5) Sensitivity to land-cover dataset is the highest in central and eastern Texas (east of −99.5°E), where there is up to a 6.3-fold difference between the modeled BVOC flux when different datasets are used. (6) Variation

between emissions estimates is especially pronounced in major metropolitan areas, where ozone pollution significantly degrades urban air quality. (7) Different specifications of bare-soil fraction can have a significant indirect effect on modeled actual BVOC flux (up to 16% of inherent BVOC flux) through modification of state variables that control vegetation temperature; however, we do not know whether the modeled indirect effects are model artifacts or representations of reality.

Urban planners and air-quality managers who make use of LSM-based model predictions of BVOC emissions should be aware of the significant sensitivity of modeled BVOC flux estimates to uncertainty in the land-cover dataset used. When LSMs are linked to climate models, this sensitivity may propagate uncertainty to all BVOC-related radiative, carbon cycle, and atmospheric-chemistry processes. Although our results focus specifically on the simulation of biogenic emissions within LSMs, they apply broadly to any application of an LSM in which the variable of interest depends in part on land-cover dataset used.

Acknowledgments

We thank Peter Lawrence, who provided us with the satellite-derived land-cover dataset and who lent us many useful insights. We are also grateful for the insightful input of Enrique Rosero and for additional constructive comments made by two anonymous reviewers, Alan Robock, and Mark Estes. This work was funded by the U.S. Environmental Protection Agency's Science To Achieve Results (STAR) Program Grant #RD83145201 and by the National Science Foundation. We thank the Texas Advanced Computing Center for computing resources.

References

Altshuller, P., 1991. The production of carbon monoxide by the homogeneous NOx-induced photooxidation of volatile organic compounds in the troposphere. Journal of Atmospheric Chemistry 13, 155–182.

Andreae, M.O., Crutzen, P.J., 1997. Atmospheric aerosols: biogeochemical sources and role in atmospheric chemistry. Science 276, 1052–1058.

Beck, M.B., 1987. Water quality modeling: a review of the analysis of uncertainty. Water Resources Research 23 (8), 1393–1442.

Bonan, G.B., Levis, S., Kergoat, L., Oleson, K.W., 2002a. Landscapes as patches of plant functional types: an integrating concept for climate and ecosystem models. Global Biogeochemistry Cycles 16.

Bonan, G.B., Oleson, K.W., Vertenstein, M., Levis, S., Zeng, X.B., Dai, Y.J., Dickinson, R.E., Yang, Z.L., 2002b. The land surface climatology of the community land model coupled to the NCAR community climate model. Journal of Climate 15, 3123–3149.

Byun, D.W., Kim, S., Czader, B., Nowak, D., Stetson, S., Estes, M., 2005. Estimation of biogenic emissions with satellite-derived land use and land-cover data for air-quality modeling of Houston-Galveston ozone nonattainment area. Journal of Environmental Management 75, 285–301.

Claeys, M., Graham, B., Vas, G., Wang, W., Vermeylen, R., Pashynska, V., Cafmeyer, J., Guyon, P., Andreae, M.O., Artaxo, P., Maenhaut, W., 2004. Formation of secondary organic aerosols through photooxidation of isoprene. Science 303, 1173–1176.

Funk, J.L., Jones, C.G., Gray, D.W., Throop, H.L., Hyatt, L.A., Lerdau, M.T., 2005. Variation in isoprene emission from Quercus rubra: sources, causes, and consequences for estimating fluxes. Journal of Geophysical Research 110, D04301.

Grell, G.A., Peckham, S.E., Schmitz, R., McKeen, S.A., Frost, G., Skamarock, W.C., Eder, B., 2005. Fully coupled "online" chemistry within the WRF model. Atmospheric Environment 39, 6957–6975.

Guenther, A., 2002. The contribution of reactive carbon emissions from vegetation to the carbon balance of terrestrial ecosystems. Chemosphere 49, 837–844.

Guenther, A., 1997. Seasonal and spatial variations in natural volatile organic compound emissions. Ecological Applications 7, 34–45.

Guenther, A., et al., 2006. Estimates of global terrestrial isoprene emissions using MEGAN (Model of Emissions of Gases and Aerosols from Nature). Atmospheric Chemistry and Physics 6, 3181–3210.

Guenther, A., Hewitt, C.N., Erickson, D., Fall, R., Geron, C., Graedel, T., Harley, P., Klinger, L., Lerdau, M., McKay, W.A., Pierce, T., Scholes, B., Steinbrecher, R., Tallamraju, R., Taylor, J., Zimmerman, P., 1995. A global model of natural volatile organic-compound emissions. Journal of Geophysical Research 100, 8873–8892.

Guenther, A., Zimmerman, P., Wildermuth, M., 1994. Natural volatile organic-compound emission rate estimates for the United-States woodland landscapes. Atmospheric Environment 28, 1197–1210.

Gulden, L.E., Yang, Z.L., 2006. Development of species-based, regional emission capacities for simulation of biogenic volatile organic compound emissions in land-surface models: an example from Texas, USA. Atmospheric Environment 40, 1464–1479.

Gulden, L.E., Yang, Z.-L., Niu, G.-Y., 2007. Interannual variation in biogenic emissions on a regional scale. Journal of Geophysical Research 112, D14103.

Hanna, S.R., Russell, A.G., Wilkinson, J.G., Vukovich, J., Hansen, D.A., 2005. Monte Carlo estimation of uncertainties in BEIS3 emission outputs and their effects on uncertainties in chemical transport model predictions. Journal of Geophysical Research 110, D01302.

Junquera, V., Russell, M.M., Vizuete, W., Kimura, Y., Allen, D., 2005. Wildfires in eastern Texas in August and September

2000: emissions, aircraft measurements, and impact on photochemistry. Atmospheric Environment 39, 4983–4996.

Kavouras, I.G., Mihalopoulos, N., Stephanou, E.G., 1998. Formation of atmospheric particles from organic acids produced by forests. Nature 395, 683–686.

Kroll, J.H., Ng, N.L., Murphy, S.M., Flagan, R.C., Seinfeld, J.H., 2006. Secondary organic aerosol formation from isoprene photooxidation. Environmental Science and Technology 40, 1869–1877.

Lawrence, P.J., Chase, T.N., 2007. Representing a new MODIS consistent land surface in the community land model (CLM 3.0). Journal of Geophysical Research 112, doi:10.1029/2006JG000168.

Levis, S., Wiedinmyer, C., Bonan, G.B., Guenther, A., 2003. Simulating biogenic volatile organic compound emissions in the community climate system model. Journal of Geophysical Research 108.

Mesinger, F., DiMego, G., Kalnay, E., Mitchell, K., Shafran, P.C., Ebisuzaki, W., Jovic, D., Woollen, J., Rogers, E., Berbery, E.H., Ek, M.B., Fan, Y., Grumbine, R., Higgins, W., Li, H., Lin, Y., Manikin, G., Parrish, D., Shi, W., 2006. North American regional reanalysis. Bulletin American Meteorological. Society 87, 343–360.

Oleson, K.W., Dai, Y., Bonan, G., Bosilovich, M., Dickinson, R., Dirmeyer, P., Hoffman, F., Houser, P., Levis, S., Niu, G.-Y., Thornton, P., Vertenstein, M., Yang, Z.-L., Zeng, X., 2004. Technical Description of the Community Land Model, National Center for Atmospheric Research, Boulder, Colorado, 174pp., Accessed at 〈http://www.cgd.ucar.edu/tss/clm/distribution/clm3.0/TechNote/CLM_Tech_Note.pdf〉www.cgd.ucar.edu/tss/clm/distribution/clm3.0/TechNote/CLM_Tech_Note.pdf.

Saltelli, A., Chan, K., Scott, E.M., 2000. Sensitivity Analysis. Wiley, England West Sussex PO19 8SQ.

Schuh, G., Heiden, A.C., Hoffmann, T., Kahl, J., Rockel, P., Rudolph, J., Wildt, J., 1997. Emissions of volatile organic compounds from sunflower and beech: dependence on temperature and light intensity. Journal of Atmospheric Chemistry 27, 291–318.

Simpson, D., Winiwarter, W., Borjesson, G., Cinderby, S., Ferreiro, A., Guenther, A., Hewitt, C.N., Janson, R., Khalil, M.A.K., Owen, S., Pierce, T.E., Puxbaum, H., Shearer, M., Skiba, U., Steinbrecher, R., Tarrason, L., Oquist, M.G., 1999. Inventorying emissions from nature in Europe. Journal of Geophysical Research 104, 8113–8152.

Smiatek, G., Bogacki, M., 2005. Uncertainty assessment of potential biogenic volatile organic compound emissions from forests with the Monte Carlo method: case study for an episode from 1 to 10 July 2000 in Poland. Journal of Geophysical Research 110, D23304.

Tao, Z., Larson, S.M., Wuebbles, D.J., Williams, A., Caughey, M., 2003. A summer simulation of biogenic contributions to ground-level ozone over the continental United States. Journal of Geophysical Research 108 (D14), 4404.

Tian, Y., Dickinson, R.E., Zhou, L., Shaikh, M., 2004. Impact of new land boundary conditions from moderate resolution imaging spectroradiometer (MODIS) data on the climatology of land-surface variables. Journal of Geophysical Research 109, D20115.

Wagener, T., Gupta, H.V., 2005. Model identification for hydrological forecasting under uncertainty. Stochastic Environmental Research Risk Assessment 19.

Wiedinmyer, C., Guenther, A., Estes, M., Strange, I.W., Yarwood, G., Allen, D.T., 2001. A land use database and examples of biogenic isoprene emission estimates for the state of Texas, USA. Atmospheric Environment 35, 6465–6477.

Yarwood, G., Wilson, G., Emery, C., Guenther, A., 1999. Development of GloBEIS—a state of the science biogenic emissions modeling system, Final Report, Prepared for Texas Natural Resource Conservation Commission, provided by the author.

Zhang, X.S., Mu, Y.J., Song, W.Z., Zhuang, Y.H., 2000. Seasonal variations of isoprene emissions from deciduous trees. Atmospheric Environment 34, 3027–3032.